

1 **Coexistence Nexus in practice: Operationalizing One Health across agroecological**
2 **landscapes and zoonotic risk in Central America**

3
4
5 Voinson M.^{1†}, Crespín S.J.^{2,3*}, Escobar D.^{4*} Moreno M.^{5*}, Castillo L.⁵, Coto Hernandez E.M.⁵, García-
6 Villata J.E.², Gonzales Perez A.M.⁶, Rios R.⁵, Romero K.⁴, Sorto V.⁴, Mejía Valencia J.G.⁶, Combe M.⁷,
7 Gozlan R.E.^{7†}

8
9 ¹ EVECO group, Univ. of Antwerp, Antwerp, Belgium

10 ² Instituto de Investigaciones Tropicales de El Salvador, El Salvador

11 ³ Escuela de Medicina Veterinaria, Facultad de Medicina Veterinaria y Agronomía, Universidad de las
12 Americas, Santiago, Chile

13 ⁴ Universidad Evangélica de El Salvador (UEES), San Salvador, El Salvador

14 ⁵ Facultad de Ciencias Naturales, Universidad de El Salvador (UES), San Salvador, El Salvador

15 ⁶ Centro de Investigaciones y Desarrollo en Salud (CENSALUD), Universidad de El Salvador (UES),
16 San Salvador, El Salvador

17 ⁷ ISEM, Univ Montpellier, CNRS, IRD, Montpellier, France

18
19
20 *Equally contributing authors

21 † Corresponding authors marina.voinson@uantwerpen.be ; rudy.gozlan@ird.fr

22
23
24 Keywords: Planetary Health, Zoonosis, Environmental Change, Conservation

25 **Abstract**

26

27 Reconciling biodiversity conservation, agricultural systems, and human health remains a central
28 sustainability challenge, yet these dimensions are often addressed in isolation. Here, we extend
29 coexistence theory beyond its traditional focus on biodiversity conservation by integrating agricultural
30 production and zoonotic risk within a One Health perspective. In doing so, we link biodiversity, food
31 production systems, land-use dynamics, and disease emergence within a common spatially explicit
32 analytical framework. Using Central America as a case study, we combine multi-pathogen occurrence
33 data with spatial indicators of anthropogenic pressure, livestock density, biodiversity, and climate in a
34 Bayesian spatiotemporal modeling framework to identify patterns of zoonotic emergence. Our results
35 reveal strong spatial clustering of emergence risk and highlight non-linear relationships, particularly
36 with livestock density, indicating that zoonotic emergence arises from interacting socio-ecological
37 pressures rather than isolated drivers. We further identify convergence zones where environmental
38 change, agricultural systems, and host diversity overlap, generating elevated levels of socio-ecological
39 vulnerability. Importantly, we show that spatial integration of these dimensions provides a tractable
40 approach for operationalizing the coexistence framework, allowing the identification of high-priority
41 areas for surveillance and intervention. While our analysis focuses on environmental and production-
42 related indicators rather than the full multidimensional scope of food security, it captures key interfaces
43 through which biodiversity, agriculture, and health interactions unfold. Overall, this study demonstrates
44 how integrating spatial epidemiology with social-ecological theory can help identify leverage points for
45 reducing zoonotic risk while supporting more resilient and sustainable landscapes. By grounding the
46 One Health perspective in spatially explicit analysis, it offers a practical pathway for informing land-
47 use planning and regional disease surveillance strategies.

48

49 **1. Introduction**

50 Reconciling biodiversity conservation with agricultural development and human health has emerged as
51 one of the defining sustainability challenges of the 21st century. Nowhere is this tension more acute than
52 in Central America, a region simultaneously marked by exceptional biological richness and persistent
53 socioeconomic vulnerability. The continued expansion of agricultural frontiers into some of the globe's
54 most biodiverse regions brings human populations, livestock systems, and wildlife communities into
55 increasingly close contact, creating conditions that heighten exposure to zoonotic diseases (Jones, et al.
56 2013; Tajudeen, et al. 2022), while also exacerbating existing structural pressures such as food insecurity
57 and governance limitations (Sibrian, et al. 2021; King, et al. 2016; Xavier, et al. 2022). The convergence
58 of these processes not only threatens the integrity of ecological systems, but also generates complex
59 geographies of risk whose impacts extend beyond national borders.

60 Central America's mosaic of ecosystems, from humid tropical forests to dry corridors, highland cloud
61 forests, and extensive agroecosystems, forms a dynamic interface where environmental change,
62 agricultural practices, and health risks intersect. These diverse landscapes host a wide range of biological
63 communities, many of which act as reservoirs for pathogens with zoonotic potential. At the same time,
64 land-use change, livestock distribution, and climatic variability reshape patterns of human-animal
65 interaction and environmental suitability, influencing the conditions under which disease emergence
66 occurs. Understanding these intertwined dynamics requires moving beyond isolated perspectives and
67 instead examining how ecological and agricultural systems jointly structure zoonotic risk.

68 Recent conceptual advances in the study of social-ecological systems offer a useful entry point for
69 addressing this challenge. Building on work that frames agroecological landscapes as dynamic systems
70 capable of existing in alternative states, ranging from conflict to coexistence, researchers have
71 introduced the notion of "coexistence parameters" (Crespin et Simonetti 2020), referring to the social
72 and ecological factors that can be managed to reduce biodiversity impacts or increase tolerance to them,
73 thereby shifting systems toward states where agricultural production and biodiversity conservation can
74 be jointly maintained (Jouzi, Leung et Nelson 2022). Expanding on this perspective, Crespin and
75 Moreira-Arce (2026) outline an agroecological systems model of coexistence in which these dimensions
76 are multidimensional and dynamically interacting. However, the role of zoonotic risk remains

77 insufficiently integrated within this framework (Hirst et Halsey 2023), despite growing evidence that
78 the same drivers shaping biodiversity and agricultural systems also influence pathogen emergence
79 (Case, et al. 2022).

80 For example, forest fragmentation can simultaneously reduce ecosystem services, displace wildlife
81 hosts, and increase human exposure to vectors (Ortiz, et al. 2021). Likewise, livestock systems may
82 amplify transmission processes by increasing host density and contact rates (Klous, et al. 2016), while
83 certain agroecological configurations may instead buffer disease transmission through the maintenance
84 of ecological interactions that regulate pathogen circulation. These processes suggest that zoonotic
85 emergence is not driven by single factors, but by constellations of interacting pressures unfolding across
86 space and time. More importantly, this challenge extends beyond the traditional One Health perspective.

87 While One Health has long emphasized the interconnections between human, animal, and environmental
88 health, less attention has been paid to how food production systems interact simultaneously with
89 biodiversity conservation and zoonotic risk. We argue that agricultural production is not merely a
90 background driver of environmental change but a central component of socio-ecological systems that
91 shapes both ecosystem integrity and disease emergence. Integrating these dimensions within a common
92 frameworks therefore represents a critical step toward understanding sustainability challenges through
93 a broader food systems and Planetary Health perspective.

94 Here, we examine the regional diversity of Central America both as a challenge and as an opportunity
95 for operationalizing this integrated perspective. Despite shared ecological continuities, each country
96 exhibits distinct combinations of land-use change, agricultural practices, governance structures, and
97 health system capacities. These differences shape not only national vulnerabilities but also
98 transboundary dynamics of risk. Vector-borne diseases such as dengue or chikungunya do not respect
99 political borders (Charles, et al. 2021), just as ecological processes extend beyond them. Similarly, land-
100 use changes in one country may alter disease ecology across a wider region (Ortiz, et al. 2021), while
101 agricultural and socioeconomic pressures can reshape exposure pathways through migration dynamics
102 (Dodd, et al. 2020). A regional and spatially explicit perspective is therefore essential.

103 Our analysis builds on this foundation to bridge conceptual and empirical approaches. Specifically, we
104 investigate how environmental conditions, agricultural systems, and ecological communities jointly

105 structure the spatial distribution of zoonotic disease emergence, and where these factors converge to
106 generate socio-ecological vulnerability hotspots. To do so, we combine spatial indicators of land use,
107 livestock density, biodiversity, climate, and anthropogenic pressure with multi-pathogen occurrence
108 data within a Bayesian spatiotemporal modeling framework.

109 While this approach does not directly capture all dimensions of food security (such as access, utilization,
110 or stability) it provides a tractable representation of the environmental and production contexts in which
111 interactions between biodiversity, agriculture, and health take place. By linking these dimensions
112 through spatial analysis, we translate the coexistence framework into an operational tool capable of
113 identifying areas where risks accumulate and interventions may have the greatest impact.

114 Ultimately, this study contributes to bridging the gap between conceptual innovation and applied
115 sustainability research. By explicitly integrating zoonotic dynamics within a coexistence perspective
116 and grounding the analysis in spatially explicit data, we provide a more coherent understanding of how
117 socio-ecological systems shape disease emergence. In doing so, we highlight opportunities to design
118 interventions that are better aligned with the complexity of real-world landscapes, where biodiversity
119 conservation, agricultural practices, and human health are inextricably connected.

120 **2. Methods**

121 **Study design and analytical framework**

122 To investigate how environmental conditions, agricultural systems, and ecological communities jointly
123 shape zoonotic disease emergence, we adopted a spatially explicit analytical framework linking multi-
124 pathogen occurrence data with indicators of land use, livestock distribution, biodiversity, and climate.

125 The analysis was structured to address two complementary objectives: (i) identifying the environmental
126 correlates of zoonotic emergence across pathogens, and (ii) examining how these relationships translate
127 into risk for a focal species with well-known ecological dynamics.

128 This approach combines a regional, multi-pathogen perspective with a species-specific analysis,
129 allowing us to capture both generalizable patterns and pathogen-specific mechanisms within a consistent
130 modeling framework.

131 **Study area and data sources**

132 The study was conducted across six Central American countries (Belize, Costa Rica, El Salvador,
133 Guatemala, Honduras, and Nicaragua), forming a biologically rich and environmentally heterogeneous
134 region. This area spans tropical lowlands, intensively cultivated agricultural landscapes, densely
135 populated urban corridors, and mountainous forested ecosystems. The climate is predominantly tropical,
136 with marked wet and dry seasons shaped by altitudinal gradients and contrasting oceanic influences.
137 Land-use patterns vary widely, ranging from expanding croplands and peri-urban settlements to
138 protected forests and coastal wetlands, creating a dynamic interface between human, livestock, and
139 wildlife populations.

140 To represent this diversity, we integrated spatially explicit covariates from multiple open-access data
141 sources (Supplementary Information 1), including socio-demographic indicators (NASA SEDAC,
142 WCS), land-cover and vegetation metrics (Sentinel-2), crop distributions (MapSPAM), livestock
143 densities (Global Livestock of the World), climatic variables (NASA POWER), and wildlife richness
144 layers (IUCN). Together, these datasets characterize the main environmental and agroecological
145 gradients shaping human–animal–environment interactions across the region. While these variables do
146 not directly capture all dimensions of food security, they provide consistent proxies for the configuration
147 and intensity of production systems, which represent key interfaces through which zoonotic risks
148 emerge.

149 Zoonotic occurrence data were obtained from the OMSA–WAHIS database (Supplementary
150 Information S11), including records for 21 pathogens over a 21-year period (2005–2025). Within this
151 framework, we conducted a focused analysis of the New World screwworm fly (*Cochliomyia*
152 *hominivorax*), a parasitic species strongly dependent on climatic conditions, livestock availability, and
153 land-use patterns. This species provides a biologically grounded case study for examining how regional
154 drivers translate into risk for a specific pathogen of major veterinary and economic relevance.

155 **Spatiotemporal data structure**

156 All variables were harmonized onto a regular 10 × 10 km grid, with each grid cell evaluated annually
157 over a 21-year period (2005–2025), forming a consistent cell–year panel for analysis. Zoonotic disease
158 occurrence was represented as yearly counts of reported outbreaks aggregated to each grid cell. Cells
159 with no reported events were retained to represent background environmental conditions,

160 acknowledging that these observations may reflect both true absence and variability in detection or
161 reporting intensity.

162 Climatic variables (mean temperature, total precipitation, and wind speed) were derived at annual
163 resolution, allowing direct temporal alignment with outbreak data. Other environmental and socio-
164 demographic variables were available at discrete time points. For these datasets—including population
165 density, land cover, crop distributions, livestock densities, and the Human Footprint Index—annual
166 values were assigned based on the closest available year. This approach preserves the structure of the
167 original datasets while avoiding the introduction of artificial trends through interpolation, resulting in
168 covariates that evolve stepwise over time and capture medium-term changes in land use and agricultural
169 systems. Wildlife richness was treated as time-invariant, reflecting longer-term ecological patterns.

170 All variables were standardized (z-scores) prior to analysis. The final dataset consisted of 9,169 grid
171 cells observed over 21 years, yielding a harmonized spatiotemporal panel of environmental conditions
172 and zoonotic emergence events.

173 **Statistical modeling approach**

174 To quantify the relationship between environmental factors and zoonotic emergence, we implemented
175 a Bayesian hierarchical modeling framework using the Integrated Nested Laplace Approximation
176 (INLA). Given the count nature of outbreak data and their strong overdispersion, observations were
177 modeled using a negative binomial distribution.

178 Let Y_i denote the number of outbreaks observed in grid cell i . The response was modeled as:

$$180 \quad Y_i \sim \text{Negative Binomial}(\lambda_i, \kappa)$$

179 where λ_i is the expected number of outbreaks and κ is the dispersion parameter.

181 The log-expected value was specified as:

$$183 \quad \log(\lambda_i) = \alpha + \sum_{j=1}^p \beta_j X_{ij} + r_i + v_i + u(t_i)$$

182
184 where α is the intercept, X_{ij} are the standardized covariates, and β_j their coefficients. The term r_i
185 represents unstructured random effects capturing residual heterogeneity, while v_i models spatially

186 structured variation. Temporal dynamics are captured through $u(t_i)$, specified as a first-order random
187 walk (RW1), which accounts for residual interannual variation not explained by the time-varying
188 covariates included in the model.

189 Spatial dependence was modeled using the stochastic partial differential equation (SPDE) approach,
190 which approximates a continuous Gaussian random field through a triangulated mesh. Priors for spatial
191 and temporal components were defined using penalized complexity priors, favoring simpler structures
192 unless supported by the data.

193 To limit multicollinearity, we retained one representative variable for each major climatic dimension
194 based on variance inflation factor (VIF) analysis, selecting mean temperature, precipitation, and
195 maximum wind speed.

196 **Spatial modeling and mesh construction**

197 The spatial field was defined over a triangulated mesh covering the study area. Mesh construction
198 followed a two-step procedure, with vertices placed at sampling locations and additional nodes added
199 to ensure full spatial coverage and minimize boundary effects.

200 An initial spatial range of 400 km was selected to capture regional-scale patterns of zoonotic emergence.
201 Inner and outer mesh resolutions were defined proportionally to this range to balance spatial precision
202 and computational efficiency. Sensitivity analyses using alternative ranges (100 km and 700 km) yielded
203 consistent results, supporting the robustness of the selected configuration.

204 **Model evaluation and predictive performance**

205 Predictive performance was evaluated using a five-fold cross-validation scheme, with 80% of the data
206 used for training and 20% for testing in each fold. Performance was assessed using the log pseudo-
207 marginal likelihood (LPML), derived from conditional predictive ordinates, as a measure of out-of-
208 sample predictive ability.

209 Discriminative performance was further evaluated using the Area Under the Receiver Operating
210 Characteristic Curve (AUROC) and the Area Under the Precision-Recall Curve (AUPRC), the latter
211 being particularly informative given the rarity of emergence events ($\approx 0.53\%$ of observations).
212 Confidence intervals were obtained via bootstrap resampling.

213 To reflect operational constraints, model performance was also assessed using ranked-risk thresholds
214 corresponding to the top 1% and top 5% of predicted high-risk locations. For each threshold, we
215 calculated precision, recall, lift, and the number of true positives detected per unit of inspection effort,
216 providing a surveillance-oriented interpretation of model outputs.

217 Separate evaluations were conducted for the full multi-pathogen dataset (all-zoonoses model) and for
218 the subset of *C. hominivorax* observations, enabling both general and pathogen-specific assessments.

219 **Inference and interpretation**

220 Model outputs are reported as posterior means and 95% Bayesian credible intervals. To facilitate
221 interpretation, regression coefficients were transformed into relative risks (RR), representing the
222 multiplicative change in expected outbreak counts associated with a one-unit increase in each
223 standardized covariate.

224 Effects were considered statistically supported when the 95% credible interval did not overlap zero (or
225 one for RRs). Given the observational nature of the data, estimated relationships are interpreted as
226 statistical associations rather than direct causal effects.

227 **3. Results**

228 **Model performance** was evaluated separately for two complementary modeling frameworks: (i) the
229 all-zoonoses model, which integrates emergence data across multiple pathogens to identify broad
230 environmental correlates of zoonotic risk, and (ii) the *C. hominivorax* model, a species-specific analysis
231 examining the determinants of emergence for this focal parasite.

232 For the all-zoonoses framework, model performance was compared across spatial configurations using
233 neighborhood radii of 100, 400, and 700 km, with year included as a fixed covariate in all cases (Table
234 2). Predictive performance was consistent across spatial scales, with similar LPML values and
235 discrimination metrics (AUROC \approx 0.89; AUPRC \approx 0.12). The 400 km configuration was retained for
236 inference, as it provided the most stable LPML estimate while capturing regional-scale spatial structure
237 in reported emergence patterns. Results from this model are used to characterize general associations
238 between environmental conditions and zoonotic occurrence across pathogens.

239 For *C. hominivorax*, predictive performance improved when cattle density was modeled as a non-linear
240 RW2 effect. The 400 km RW2 specification yielded the highest predictive accuracy among species-

241 specific models (AUROC = 0.97–0.98; AUPRC = 0.26). Because this model was fitted to a restricted
242 dataset of confirmed cases, its LPML values are not directly comparable to those of the all-zoonoses
243 model; however, the discrimination metrics indicate a strong ability to identify high-risk locations for
244 this species.

245 Together, these models provide complementary perspectives: the all-zoonoses model captures general
246 patterns of zoonotic emergence at the regional scale, while the *C. hominivorax* model characterizes
247 species-specific spatial responses within the same environmental context. All subsequent analyses,
248 including fixed-effect estimates, spatial predictions, and temporal patterns, are therefore based on the
249 selected 400 km configurations.

250 **Fixed covariates**

251 Fixed-effects results indicate that climatic and ecological variables show the strongest associations with
252 zoonotic disease occurrence across livestock systems, whereas socio-demographic factors and most
253 land-cover variables display weaker or more uncertain relationships (Tables 3–4).

254 In the all-zoonoses model, temperature exhibits a negative association with emergence risk (posterior
255 mean = -0.35 ; RR = 0.71, 95% BCI: 0.68–0.74), while precipitation shows a positive association
256 (posterior mean = 0.25; RR = 1.29, 95% BCI: 1.18–1.41). Wind speed presents a weak and uncertain
257 effect (posterior mean = 0.05; RR = 1.05, 95% BCI: 0.82–1.36). Mammal–bird richness is positively
258 associated with emergence risk (posterior mean = 0.76; RR = 2.13, 95% BCI: 1.43–3.18).

259 Among anthropogenic variables, cropland shows a modest negative association (posterior mean = -0.21 ;
260 RR = 0.81, 95% BCI: 0.67–0.97), whereas built-up and water areas show no statistically supported
261 effects. Population density is not associated with emergence risk (posterior mean = -0.08 ; RR = 0.92,
262 95% BCI: 0.78–1.10), while the Human Footprint Index displays a strong positive association (posterior
263 mean = 0.78; RR = 2.19, 95% BCI: 1.61–2.99). This relationship may reflect a combination of increased
264 environmental pressure and heterogeneity in surveillance or reporting intensity across the region.

265 The pathogen-specific *C. hominivorax* model (Table 4) shows broadly similar patterns, with stronger
266 effect sizes for several covariates. Temperature shows a more pronounced negative association
267 (posterior mean = -0.55 ; RR = 0.57, 95% BCI: 0.53–0.62), and precipitation a stronger positive

268 association (posterior mean = 0.28; RR = 1.32, 95% BCI: 1.18–1.49). Mammal–bird richness is also
269 positively associated with emergence (posterior mean = 1.01; RR = 2.75, 95% BCI: 1.52–5.06).
270 In contrast, socio-demographic and most land-cover variables show weak or uncertain effects, with the
271 exception of cropland, which retains a negative association (posterior mean = –0.23; RR = 0.79, 95%
272 BCI: 0.63–0.99). The Human Footprint Index also shows a positive but more moderate association
273 (posterior mean = 0.59; RR = 1.81, 95% BCI: 1.14–2.88).
274 Across both models, climatic conditions and wildlife richness show the most consistent associations
275 with reported zoonotic occurrence, while anthropogenic variables exhibit more variable effects. The
276 species-specific model for *C. hominivorax* displays stronger and more structured responses to these
277 gradients, consistent with its narrower ecological niche.

278 **Identifying emergence risk**

279 Across the study region, both the all-zoonoses model and the *Cochliomyia hominivorax*–specific model
280 show similar large-scale spatial patterns, with elevated emergence risk concentrated in southern Mexico,
281 Guatemala, Honduras, and Nicaragua (Figures 1–2). In both models, these high-risk areas are associated
282 with low spatial uncertainty and narrow 95% credible intervals, indicating strong model support.
283 Differences emerge in the spatial extent and definition of predicted hotspots. The all-zoonoses model
284 shows a broader distribution of elevated risk, accompanied by greater uncertainty in peripheral regions.
285 In contrast, the *C. hominivorax* model identifies more spatially concentrated hotspots with sharper
286 boundaries. Combining predicted risk with uncertainty allows the identification of both reliable hotspots
287 (i.e. areas of high risk and low uncertainty) and more uncertain hotspots, where elevated risk is
288 associated with wider credible intervals. Outside these areas, predicted risk remains low and shows
289 limited spatial structure. These spatial patterns are consistent with threshold-based classification results
290 (Table S1). The top 1% risk threshold identifies a small number of high-precision hotspots, whereas the
291 top 5% threshold captures a larger number of areas with lower certainty.

292 **Non-linear relationship with cattle density.** Livestock-related emergence risk shows a pronounced
293 non-linear association with cattle density across all models (Figure 3). For all zoonotic events combined
294 (Figure 3A), the estimated effect increases sharply at low cattle densities, reaches a maximum at
295 intermediate densities (approximately 80,000–100,000 animals), and then declines at higher densities.

296 This decline is accompanied by wider credible intervals, indicating greater uncertainty at very high cattle
297 concentrations.

298 A similar pattern is observed in the *C. hominivorax* model (Figure 3B), with a steeper increase toward
299 the peak and a more pronounced decline at higher densities. Overall, these results may indicate that
300 intermediate cattle densities are associated with higher levels of reported emergence, whereas both low-
301 density and high-density systems show lower estimated risk.

302 **Temporal effect**

303 Temporal dynamics differ between the all-zoonoses and the *C. hominivorax* models (Figure 4). In the
304 all-zoonoses model (Figure 4A), the temporal random effect shows moderate interannual variability with
305 an overall increasing trend across the study period. After a relatively low baseline around 2006–2008,
306 the effect increases progressively, with a more pronounced rise after 2020. This pattern suggests an
307 increase in reported zoonotic emergence over time, although it may reflect a combination of ecological
308 processes and changes in surveillance capacity or reporting practices.

309 In contrast, the *C. hominivorax* model (Figure 4B) shows a distinct temporal structure. From 2005 to
310 approximately 2018, the temporal random effect remains close to zero with wide credible intervals,
311 consistent with very low numbers of reported cases during this period. A slight fluctuation is observed
312 around 2010, but the trajectory remains generally flat until the late 2010s. Beginning around 2018–2020,
313 the temporal effect increases sharply, followed by a rapid rise in the final years of the series,
314 accompanied by narrower credible intervals.

315 Taken together, these results indicate that while reported zoonotic emergence across pathogens shows a
316 gradual increasing trend, *C. hominivorax* is characterized by a prolonged period of low occurrence
317 followed by a rapid increase in recent years. This contrast highlights differences in temporal dynamics
318 between aggregated multi-pathogen patterns and species-specific emergence signals.

319

320 **4. Discussion**

321 Our results provide empirical support for an expanded coexistence framework in which biodiversity
322 conservation, agricultural production, and health are not treated as separate policy domains but as
323 interacting components of a common socio-ecological system (König, et al. 2020; Fiasco et Massarella

324 2022; Massarella, et al. 2022). By explicitly linking zoonotic emergence to the original food-biodiversity
325 nexus, this study advances the operationalization of coexistence theory and offers a spatially explicit
326 framework for analyzing the interactions between food production systems, environmental change, and
327 disease risk. At the same time, our findings emphasize that these relationships should be interpreted as
328 statistical associations rather than direct causal mechanisms, reflecting the complexity of underlying
329 ecological and epidemiological processes.

330 Across the region, zoonotic risk is not randomly distributed but concentrated in areas where human
331 activity, livestock presence, and wildlife diversity intersect. The consistent associations observed with
332 the Human Footprint Index, cattle density, and mammal-bird richness point to these interfaces as
333 recurrent conditions under which emergence becomes more likely (Mancini, et al. 2024; Barreto et Prist
334 2025). From a One Health perspective, these zones correspond to areas where interactions among
335 human, animal, and environmental health are intensified. However, part of these patterns may also
336 reflect variation in surveillance effort and reporting capacity, particularly in areas with higher human
337 footprint, where detection systems are more developed. Distinguishing between biological risk and
338 detection bias therefore remains a key challenge for interpretation.

339 Our findings further reveal asymmetries among coexistence parameters, with some pressures amplifying
340 risk and others potentially mitigating it. While higher human footprint is associated with increased
341 emergence risk (RR = 2.19), cropland cover shows a modest negative relationship (RR = 0.81),
342 suggesting that not all anthropogenic transformations have equivalent effects. One interpretation is that
343 differences in land-use configuration, rather than simple intensity, shape the degree of human-animal
344 contact and environmental disturbance. At the same time, the positive association with wildlife richness
345 (RR = 2.13) highlights a well-known tension in disease ecology: biodiverse systems may both sustain
346 ecological functions and provide reservoirs for pathogen persistence. However, this pattern should be
347 interpreted cautiously, as species richness does not directly capture host competence or transmission
348 pathways, and may also correlate with unobserved environmental gradients.

349 More broadly, the relatively weak and inconsistent effects observed for several land-use and crop-
350 specific variables suggest that zoonotic emergence is unlikely to be driven by single factors in isolation
351 (Chaves, et al. 2022). Instead, it appears to arise from particular constellations of pressures acting

352 simultaneously across space and time (Jagadesh, Combe et Gozlan 2022). From this perspective,
353 coexistence can be understood not as a fixed outcome, but as a dynamic position within a
354 multidimensional socio-ecological space (Combs, et al. 2021; Crespín et Simonetti 2020), where
355 systems may shift toward more stable or more vulnerable configurations depending on how these
356 pressures interact.

357 The non-linear relationship observed with cattle density illustrates this complexity particularly clearly.
358 Risk increases sharply at low to intermediate densities before declining at higher densities, a pattern that
359 is especially pronounced for *C. hominivorax*. This species-specific response is consistent with its
360 biology as an obligate parasite dependent on host availability (Long, et al. 2026). At intermediate
361 densities, livestock abundance may increase host exposure and facilitate transmission, whereas at higher
362 densities the transition toward more intensive management systems (potentially including improved
363 veterinary care and vector control) may reduce infestation opportunities. However, alternative
364 explanations cannot be excluded, including differences in reporting practices between production
365 systems or unmeasured aspects of livestock management.

366 Temporal dynamics further reinforce the importance of cautious interpretation. While the all-zoonoses
367 model suggests a gradual increase in emergence over time, the sharp resurgence observed for *C.*
368 *hominivorax* after 2018-2020 aligns with its documented re-emergence following near-eradication
369 (Valdez-Espinoza, et al. 2025). At the same time, part of the observed temporal signal may reflect
370 improvements in surveillance systems, changes in reporting practices, or increased awareness, rather
371 than purely ecological processes. Disentangling these effects remains difficult in observational datasets
372 and highlights the importance of interpreting temporal trends as combined signals of biological and
373 institutional dynamics.

374 By operationalizing the coexistence framework through spatial analysis, our approach provides a
375 practical means of identifying areas where environmental pressures, agricultural systems, and disease
376 dynamics converge. These “socio-ecological vulnerability hotspots” offer a useful basis for prioritizing
377 surveillance and intervention efforts. However, it is important to note that our analysis relies primarily
378 on environmental and production-related indicators, and does not explicitly capture all dimensions of
379 food security, such as access, utilization, or stability. As a result, the identified hotspots should be

380 interpreted as areas of elevated environmental and epidemiological vulnerability rather than
381 comprehensive measures of food system outcomes.

382 However, this limitation should not obscure one of the central contributions of the framework. Beyond
383 its implications for zoonotic surveillance, our approach highlights the need to reconsider agricultural
384 production as a central component of socio-ecological sustainability rather than simply a driver of
385 environmental change. Agricultural systems are often viewed primarily through their impacts on
386 biodiversity loss and disease emergence. Yet our results suggest that the configuration of agroecological
387 landscapes can simultaneously influence biodiversity conservation, production systems, and zoonotic
388 risk. This perspective moves beyond a simple biodiversity-health linkage and instead emphasizes the
389 interconnected nature of food production, ecosystem integrity, and health outcomes within shared
390 landscapes. In this respect, the Coexistence Nexus framework aligns not only with One Health principles
391 but also with broader Planetary Health and food-system resilience agendas, where the challenge is not
392 merely to reduce disease risk, but to sustain ecological and productive systems capable of supporting
393 long-term human well-being.

394 At the policy level, the strong spatial clustering of risk underscores the limitations of uniform, region-
395 wide intervention strategies (Combs, et al. 2021). Instead, the observed heterogeneity supports more
396 targeted approaches, in which surveillance and mitigation efforts are adapted to local configurations of
397 risk. This may involve prioritizing high-certainty hotspots for intensive monitoring, while using more
398 precautionary strategies in areas where uncertainty remains high. Coordinating agricultural,
399 environmental, and public health policies within such a framework can help embed disease prevention
400 within broader sustainability strategies (Clifford Astbury, et al. 2023).

401 Finally, while Central America provides a compelling case study, the transferability of this framework
402 should be considered with caution. The specific relationships identified here are shaped by regional
403 ecological, agricultural, and institutional contexts. Nonetheless, the broader approach of linking spatial
404 epidemiology with socio-ecological theory may offer a useful template for other regions facing similar
405 interactions between biodiversity change, agricultural systems, and zoonotic risk (Mahon, et al. 2024).

406 In conclusion, this study highlights the importance of integrating a One Health perspective into analyses
407 of socio-ecological systems. Rather than representing a simple trade-off between production and

408 conservation, the coexistence nexus emerges as a dynamic system shaped by interacting environmental
409 and anthropogenic pressures. Identifying how these pressures combine to generate patterns of zoonotic
410 emergence provides a basis for more targeted and context-sensitive interventions. As such, the value of
411 this framework lies less in predicting specific outcomes than in helping to identify where and how
412 interventions may be most effective within complex and evolving landscapes.

413

414 **Acknowledgments:** S. Crespin was supported by the One Health Community of Knowledge from IRD.
415 M. Voinson, R. E. Gozlan and M. Combe were supported by the BCOMING project (Horizon Europe
416 project 101059483) from the European Union and FNRS.

417

418 **References**

- 419 (IFPRI), International Food Policy Research Institute, and International Institute For Applied
420 Systems Analysis (IIASA). "Global Spatially-Disaggregated Crop Production Statistics
421 Data for 2005 Version 3.2." *Geospatial Data* (Harvard Dataverse), 2015.
- 422 Adisasmito, Wiku B., et al. "One Health: A new definition for a sustainable and healthy future."
423 Edited by Jeffrey D. Dvorin. *PLOS Pathogens* (Public Library of Science (PLOS)) 18
424 (June 2022): e1010537.
- 425 Barrera, N. "The Transnational Capture and Pillage of Central America. Jus Semper Global
426 Alliance." *The Transnational Capture and Pillage of Central America. Jus Semper*
427 *Global Alliance*. 2024.
- 428 Case, B. K. M., Jean-Gabriel Young, Daniel Penados, Carlota Monroy, Laurent Hébert-
429 Dufresne, and Lori Stevens. "Spatial epidemiology and adaptive targeted sampling to
430 manage the Chagas disease vector *Triatoma dimidiata*." Edited by Marilia Sá Carvalho.
431 *PLOS Neglected Tropical Diseases* (Public Library of Science (PLOS)) 16 (June 2022):
432 e0010436.
- 433 Center For International Earth Science Information Network-CIESIN-Columbia University.
434 "Gridded Population of the World, Version 4 (GPWv4): Population Density, Revision
435 11." (Palisades, NY: NASA Socioeconomic Data and Applications Center (SEDAC))
436 2017.
- 437 Charles, Roxanne A., et al. "Ticks and Tick-Borne Diseases in Central America and the
438 Caribbean: A One Health Perspective." *Pathogens* (MDPI AG) 10 (October 2021):
439 1273.
- 440 Chaves, Luis Fernando, Julie Velasquez Runk, Luke R. Bergmann, and Nicole L. Gottdenker.
441 "Reifications in Disease Ecology 1: Demystifying Land Use Change in Pathogen
442 Emergence." *Capitalism Nature Socialism* (Informa UK Limited) 34 (November 2022):
443 23–39.

444 Clifford Astbury, Chloe, et al. "Policies to prevent zoonotic spillover: a systematic scoping
445 review of evaluative evidence." *Globalization and Health* (Springer Science and
446 Business Media LLC) 19 (November 2023).

447 Combe, Marine, and Rodolphe Elie Gozlan. "When the Blue Marble Health concept challenges
448 our current understanding of One Health." *One Health* (Elsevier BV) 19 (December
449 2024): 100935.

450 Combs, Matthew A., et al. "Socio-ecological drivers of multiple zoonotic hazards in highly
451 urbanized cities." *Global Change Biology* (Wiley) 28 (December 2021): 1705–1724.

452 Crespin, Silvio J., and Javier A. Simonetti. "Traversing the food-biodiversity nexus towards
453 coexistence by manipulating social–ecological system parameters." *Conservation
454 Letters* (Wiley) 14 (November 2020).

455 Crespin, Silvio, and Dario Moreira-Arce. "Creating opportunities for coexistence to overcome
456 the food–biodiversity challenge." (California Digital Library (CDL)) February 2026.

457 Díaz, Sandra, et al. "Assessing nature’s contributions to people." *Science* (American
458 Association for the Advancement of Science (AAAS)) 359 (January 2018): 270–272.

459 Dodd, Warren, et al. "Factors Associated with Seasonal Food Insecurity among Small-Scale
460 Subsistence Farming Households in Rural Honduras." *International Journal of
461 Environmental Research and Public Health* (MDPI AG) 17 (January 2020): 706.

462 Fiasco, Valentina, and Kate Massarella. "Human-Wildlife Coexistence: Business as Usual
463 Conservation or an Opportunity for Transformative Change?" *Conservation and Society
464 (Medknow)* 20 (April 2022): 167–178.

465 Fischer, Joern, et al. "Reframing the Food–Biodiversity Challenge." *Trends in Ecology &
466 Evolution* (Elsevier BV) 32 (May 2017): 335–345.

467 Gilbert, Marius, et al. "Global distribution data for cattle, buffaloes, horses, sheep, goats, pigs,
468 chickens and ducks in 2010." *Scientific Data* (Springer Science and Business Media
469 LLC) 5 (October 2018).

470 Hayek, Matthew N. "The infectious disease trap of animal agriculture." *Science Advances
471 (American Association for the Advancement of Science (AAAS))* 8 (November 2022).

472 Hirst, Kristen M., and Samniqueka J. Halsey. "Bacterial zoonoses impacts to conservation of
473 wildlife populations: a global synthesis." *Frontiers in Conservation Science* (Frontiers
474 Media SA) 4 (November 2023).

475 International Food Policy Research Institute (IFPRI). "Global Spatially-Disaggregated Crop
476 Production Statistics Data for 2010 Version 2.0." *Geospatial Data* (Harvard Dataverse),
477 2019.

478 International Food Policy Research Institute (IFPRI). "Global Spatially-Disaggregated Crop
479 Production Statistics Data for 2020 Version 2.0." *Geospatial Data* (Harvard Dataverse),
480 2024.

481 IUCN, red list. "Species richness of mammals and birds combined with AoH maps." *Species
482 richness of mammals and birds combined with AoH maps*. 2021.

483 Jagadesh, Soushieta, Marine Combe, and Rodolphe Elie Gozlan. "Human-Altered Landscapes
484 and Climate to Predict Human Infectious Disease Hotspots." *Tropical Medicine and
485 Infectious Disease* (MDPI AG) 7 (July 2022): 124.

486 Jones, Bryony A., et al. "Zoonosis emergence linked to agricultural intensification and
487 environmental change." *Proceedings of the National Academy of Sciences* (Proceedings
488 of the National Academy of Sciences) 110 (May 2013): 8399–8404.

- 489 Jouzi, Zeynab, Yu-Fai Leung, and Stacy Nelson. "Addressing the food security and
490 conservation challenges: Can be aligned instead of apposed?" *Frontiers in Conservation*
491 *Science* (Frontiers Media SA) 3 (July 2022).
- 492 King, Matthew Wilburn, Marco Antonio González Pastora, Mauricio Castro Salazar, and
493 Carlos Manuel Rodriguez. "Environmental governance and peacebuilding in post-
494 conflict Central America: Lessons from the Central American Commission for
495 Environment and Development." (Routledge) April 2016: 777–802.
- 496 Klous, Gijs, Anke Huss, Dick J. J. Heederik, and Roel A. Coutinho. "Human–livestock contacts
497 and their relationship to transmission of zoonotic pathogens, a systematic review of
498 literature." *One Health* (Elsevier BV) 2 (December 2016): 65–76.
- 499 König, Hannes J., Christian Kiffner, Stephanie Kramer-Schadt, Christine Fürst, Oliver Keuling,
500 and Adam T. Ford. "Human–wildlife coexistence in a changing world." *Conservation*
501 *Biology* (Wiley) 34 (May 2020): 786–794.
- 502 Long, Brit, Anissa Finley, Stephen Y. Liang, and Heather A. Heaton. "New world screwworm:
503 A focused review for the emergency medicine clinician." *The American Journal of*
504 *Emergency Medicine* (Elsevier BV) 102 (April 2026): 8–12.
- 505 Mahon, Michael B., et al. "A meta-analysis on global change drivers and the risk of infectious
506 disease." *Nature* (Springer Science and Business Media LLC) 629 (May 2024): 830–
507 836.
- 508 Mancini, Matheus C. S., Julia Rodrigues Barreto, Raquel L. Carvalho, Renata L. Muylaert,
509 Ricardo Corasa Arrais, and Paula R. Prist. "Landscape Ecology Meets Disease Ecology
510 in the Tropical America: Patterns, Trends, and Future Directions." *Current Landscape*
511 *Ecology Reports* (Springer Science and Business Media LLC) 9 (April 2024): 31–62.
- 512 Massarella, Kate, Judith E. Krauss, Wilhelm Kiwango, and Robert Fletcher. "Exploring
513 Convivial Conservation in Theory and Practice: Possibilities and Challenges for a
514 Transformative Approach to Biodiversity Conservation." *Conservation and Society*
515 (Medknow) 20 (April 2022): 59–68.
- 516 Morand, Serge, and Claire Lajaunie. "Outbreaks of Vector-Borne and Zoonotic Diseases Are
517 Associated With Changes in Forest Cover and Oil Palm Expansion at Global Scale." *Frontiers in Veterinary Science* (Frontiers Media SA) 8 (March 2021).
- 518 Morris, Aaron L., et al. "Deforestation-driven food-web collapse linked to emerging tropical
519 infectious disease, *Mycobacterium ulcerans*." *Science Advances* (American Association
520 for the Advancement of Science (AAAS)) 2 (December 2016).
- 521 Mulieri, Pablo Ricardo, and Luciano Damián Patitucci. "Using ecological niche models to
522 describe the geographical distribution of the myiasis-causing *Cochliomyia hominivorax*
523 (Diptera: Calliphoridae) in southern South America." *Parasitology Research* (Springer
524 Science and Business Media LLC) 118 (February 2019): 1077–1086.
- 525 Obura, David O., et al. "Integrate biodiversity targets from local to global levels." *Science*
526 (American Association for the Advancement of Science (AAAS)) 373 (August 2021):
527 746–748.
- 528 Ortiz, Diana I., Marta Piche-Ovares, Luis M. Romero-Vega, Joseph Wagman, and Adriana
529 Troyo. "The Impact of Deforestation, Urbanization, and Changing Land Use Patterns
530 on the Ecology of Mosquito and Tick-Borne Diseases in Central America." *Insects*
531 (MDPI AG) 13 (December 2021): 20.
- 532 Palmeirim, Ana Filipa, Julia Rodrigues Barreto, and Paula R. Prist. "The importance of
533 Indigenous Lands and landscape structure in shaping the zoonotic disease risk—Insights
534

535 from the Brazilian Atlantic Forest." *One Health* (Elsevier BV) 21 (December 2025):
536 101104.

537 Perfecto, Ivette, et al. "Looking beyond land-use and land-cover change: Zoonoses emerge in
538 the agricultural matrix." *One Earth* (Elsevier BV) 6 (September 2023): 1131–1142.

539 Prist, Paula Ribeiro, et al. "Promoting landscapes with a low zoonotic disease risk through forest
540 restoration: The need for comprehensive guidelines." *Journal of Applied Ecology*
541 (Wiley) 60 (June 2023): 1510–1521.

542 Sandoval, Danny Fernando, John Jairo Junca Paredes, Karen Johanna Enciso Valencia, Manuel
543 Francisco Díaz Baca, Aura María Bravo Parra, and Stefan Burkart. "Long-term
544 relationships of beef and dairy cattle and greenhouse gas emissions: Application of co-
545 integrated panel models for Latin America." *Heliyon* (Elsevier BV) 10 (January 2024):
546 e23364.

547 Service, Copernicus Land Monitoring, and Copernicus Land Monitoring Service Helpdesk.
548 "Land Cover 2020 (raster 10 m), global, annual - version 1." (Copernicus Land
549 Monitoring Service) 2025.

550 Sibrian, Ricardo, Marco d’Errico, Patricia Palma de Fulladolsa, and Flavia Benedetti-
551 Michelangeli. "Household Resilience to Food and Nutrition Insecurity in Central
552 America and the Caribbean." *Sustainability* (MDPI AG) 13 (August 2021): 9086.

553 Simon, Sabrina Soares, Marcos Amaku, and Eduardo Massad. "The spread of infectious
554 diseases in migration routes between caravans and resident communities: Modelling
555 yellow fever in Central America." *The Journal of Climate Change and Health* (Elsevier
556 BV) 24 (July 2025): 100473.

557 Sparks, Adam. "nasapower: A NASA POWER Global Meteorology, Surface Solar Energy and
558 Climatology Data Client for R." *Journal of Open Source Software* (The Open Journal)
559 3 (October 2018): 1035.

560 Tajudeen, Yusuf Amuda, Iyiola Olatunji Oladunjoye, Ousman Bajinka, and Habeebullah
561 Jayeola Oladipo. "Zoonotic Spillover in an Era of Rapid Deforestation of Tropical Areas
562 and Unprecedented Wildlife Trafficking: Into the Wild." *Challenges* (MDPI AG) 13
563 (August 2022): 41.

564 United Nations Environment Programme, (UNEP). "Helping farmers beat the climate crisis in
565 Central America’s Dry Corridor." *Helping farmers beat the climate crisis in Central*
566 *America’s Dry Corridor*. n.d.

567 Valdez-Espinoza, Uriel Mauricio, Lucas A. Fadda, Roberta Marques, Luis Osorio-Olvera,
568 Daniel Jiménez-García, and Andrés Lira-Noriega. "The reemergence of the New World
569 screwworm and its potential distribution in North America." *Scientific Reports*
570 (Springer Science and Business Media LLC) 15 (July 2025).

571 WHO. "One Health High-Level Expert Panel Annual Report." Tech. rep., WHO, 2022.

572 Wildlife Conservation Society. *Human foot print*. 2025. [https://wcshumanfootprint.org/data-
573 access](https://wcshumanfootprint.org/data-access).

574 Xavier, Luciana Yokoyama, Maila Guilhon, Leandra Regina Gonçalves, Marina Ribeiro
575 Corrêa, and Alexander Turra. "Waves of Change: Towards Ecosystem-Based
576 Management to Climate Change Adaptation." *Sustainability* (MDPI AG) 14 (January
577 2022): 1317.

578

579

580
581
582

Table 1: Standardized covariates used in the model including mean, quartiles, Median and variance inflation factor (VIF).

	Covariate	Mean	Q2.5%	Q97.5%	Median	VIF value
<i>Socio-demographic (From NASA SEDAC's and WCS)</i>	Population density (persons/km2)	0.001	-0.305	-0.003	-0.201	1.801
	HFI (/10km)	-0.025	-0.756	0.533	-0.053	2.882
<i>Land cover area (from sentinel 2)</i>	Forest (Ha)	-0.051	-0.473	-0.089	-0.373	1.294
	Water (Ha)	0.009	-0.201	-0.176	-0.199	1.309
	Built up (Ha)	-0.018	-0.557	0.131	-0.339	2.543
	Crops (Ha)	-0.016	-0.267	-0.252	-0.267	1.883
<i>Dominant crops (from MapSPAM)</i>	Banana (Ha)	-0.016	-0.135	-0.131	-0.135	1.204
	Beans (Ha)	0.055	-0.516	0.086	-0.390	1.369
	Maize (Ha)	0.059	-0.488	0.110	-0.315	1.785
	Coconut (Ha)	0.003	-0.140	-0.029	-0.140	1.054
	Palm Oil (Ha)	-0.009	-0.288	-0.195	-0.288	1.237
	Rice (Ha)	-0.026	-0.175	-0.161	-0.174	1.308
<i>Livestock's (from Global Livestock of the World, GLW)</i>	Sugar cane (Ha)	0.009	-0.206	-0.152	-0.203	2.072
	Cattle (Nb/10km)	0.017	-0.714	0.386	-0.258	1.431
	Chicken (Nb/10km)	-0.007	-0.279	-0.042	-0.223	1.398
	Sheep (Nb/10km)	0.014	-0.111	-0.073	-0.097	1.960
	Goat (Nb/10km)	0.025	-0.297	0.000	-0.180	2.224
<i>Climatic variables (from Nasa Power)</i>	Pig (Nb/10km)	0.004	-0.156	-0.043	-0.113	1.206
	Temperature (°C)	0.000	-0.609	0.755	0.213	1.771
	Precipitation (mm)	0.000	-0.739	0.736	-0.299	1.485
<i>Wild animal richness</i>	Wind speed (knots)	0.000	-0.831	0.555	-0.166	1.804
	Mammal bird richness	-0.052	-0.645	0.624	0.132	1.635

583
584

585 **Table 2:** Comparison of spatial model performance based on the logarithmic pseudo-marginal
586 likelihood (LPML) and predictive accuracy metrics. For each model, LPML, AUROC, and AUPRC
587 values are reported as medians with their associated ranges across repeated model fits. All-zoonoses
588 models were fitted using neighborhood radii of 100, 400, and 700 km to assess sensitivity to spatial
589 structure. The *C. hominivorax* models were fitted on a subsampled dataset restricted to confirmed *C.*
590 *hominivorax* cases and are therefore not directly comparable to the all-zoonoses models. Two
591 specifications are shown: one including cattle density as a fixed effect, and one modelling cattle density
592 using a non-linear RW2 effect.

593

MODEL	LPML	AUROC (IC 95)	AUPRC (IC 95)	PREVALENCE
ALL-ZOONOTIC 400	-0.03 (0.0008)	0.89 (0.88 ; 0.91)	0.12 (0.10 ; 0.14)	0.53
ALL-ZOONOTIC 100	-0.03 (0.0008)	0.89 (0.87 ; 0.91)	0.12 (0.10 ; 0.15)	0.53
ALL-ZOONOTIC 700	-0.03 (0.0008)	0.89 (0.87 ; 0.91)	0.12 (0.10 ; 0.15)	0.53
C.HOMINIVIRAX (+ CATTLE FIXED EFFECT)	-0.03 (0.02)	0.96 (0.96 ; 0.97)	0.12 (0.10 ; 0.16)	0.38
C.HOMINIVIRAX (+ CATTLE RW2 EFFECT)	-0.017 (0.0004)	0.98 (0.97 ; 0.98)	0.26 (0.23 ; 0.30)	0.38

594

595

596 **Table 3:** Posterior mean estimates, 95% Bayesian credible intervals (BCI), and corresponding relative
597 risks (RR) for socio-demographic, land-cover, livestock, climatic, and wildlife covariates included in
598 the final spatial model. Relative risks were obtained by exponentiating posterior mean coefficients and
599 represent the multiplicative change in prevalence associated with a one-unit increase in each
600 standardized covariate, holding all other variables constant. Covariates were classified as having a
601 positive or negative effect when their 95% BCI did not overlap zero (or RR did not overlap 1); effects
602 were considered non-significant otherwise.

603

	Covariate	Posterior mean	Q025	Q975	RR (95% BCI)	Significative effect
<i>Socio-demographic</i>	Population density	-0.08	-0.25	0.09	0.92 (0.78 ; 1.10)	-
	HFI	0.78	0.48	1.09	2.19 (1.61 ; 2.99)	Positive
<i>Land cover area</i>	Built up	-0.06	-0.31	0.19	0.94 (0.73 ; 1.21)	-
	Cropland	-0.21	-0.40	-0.02	0.81 (0.67 ; 0.97)	Negative
	Water	-0.17	-0.40	0.05	0.84 (0.67 ; 1.05)	-
<i>Climatic variables</i>	Temperature	-0.35	-0.39	-0.30	0.71 (0.68 ; 0.74)	Negative
	Precipitation	0.25	0.17	0.34	1.29 (1.18 ; 1.41)	Positive
	Wind speed	0.05	-0.20	0.31	1.05 (0.82 ; 1.36)	-
<i>Wild animal richness</i>	Mammal-bird richness	0.76	0.36	1.16	2.13 (1.43 ; 3.18)	Positive

604

605

606

607

608

609

610

611

612 **Table 4:** Posterior mean estimates, 95% Bayesian credible intervals (BCI), and corresponding relative
613 risks (RR) for socio-demographic, land-cover, livestock, climatic, and wildlife covariates included in
614 the final spatial model for the *C. hominivorax* case study. Relative risks were obtained by exponentiating
615 posterior mean coefficients and represent the multiplicative change in prevalence associated with a one-
616 unit increase in each standardized covariate, holding all other variables constant. Covariates were
617 classified as having a positive or negative effect when their 95% BCI did not overlap zero (or RR did
618 not overlap 1); effects were considered non-significant otherwise.

619

	Covariate	Posterior Mean	Q025	Q975	RR (95% BCI)	Significative effect
<i>Socio-demographic</i>	Population density	-0.24	-0.59	0.03	0.79 (0.55 ; 1.12)	-
	HFI	0.59	0.13	1.06	1.81 (1.14 ; 2.88)	Positive
<i>Land cover area</i>	Built up	0.14	-0.29	0.57	1.15 (0.75 ; 1.77)	-
	Cropland	-0.23	-0.46	-0.005	0.79 (0.63 ; 0.99)	Negative
	Water	-0.16	-0.44	0.12	0.85 (0.64 ; 1.13)	-
<i>Climatic variables</i>	Temperature	-0.55	-0.63	-0.48	0.57 (0.53 ; 0.62)	Negative
	Precipitation	0.28	0.16	0.40	1.32 (1.18 ; 1.49)	Positive
	Wind speed	0.12	-0.22	0.46	1.13 (0.80 ; 1.58)	-
<i>Wild animal richness</i>	Mammal-bird richness	1.01	0.42	1.62	2.75 (1.52 ; 5.06)	Positive

620
621
622
623
624
625
626

627 **Captions**

628

629 **Figure 1:** Spatial predictions of all zoonotic emergence risk and associated uncertainty. Panels

630 show (top left) the posterior mean of emergence risk estimated using the INLA model, (top right)

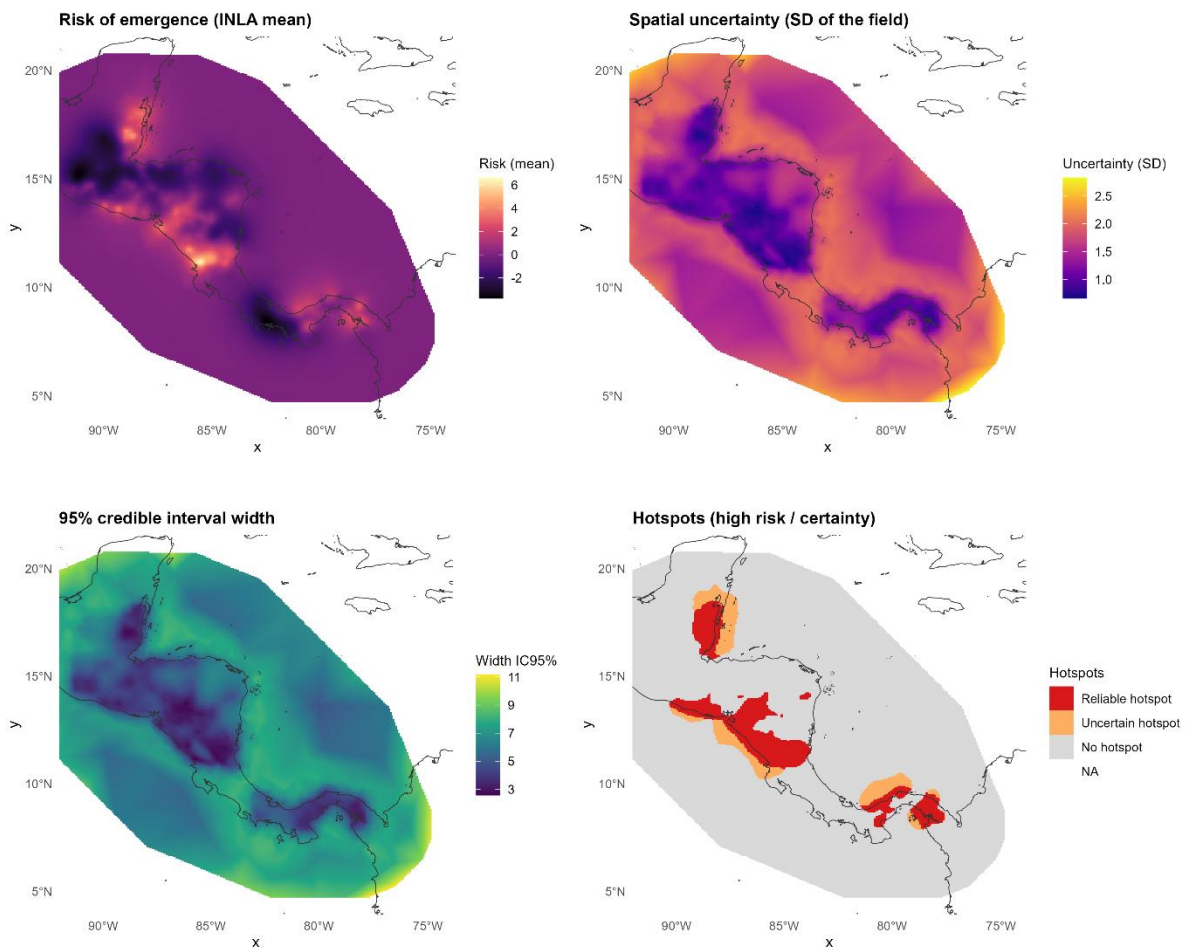
631 the spatial uncertainty expressed as the standard deviation of the latent field, (bottom left) the

632 width of the 95% credible interval, and (bottom right) the resulting hotspot classification

633 combining risk and uncertainty, distinguishing reliable hotspots (high risk and low uncertainty),

634 uncertain hotspots (high risk and high uncertainty), and areas with no detected hotspot.

635



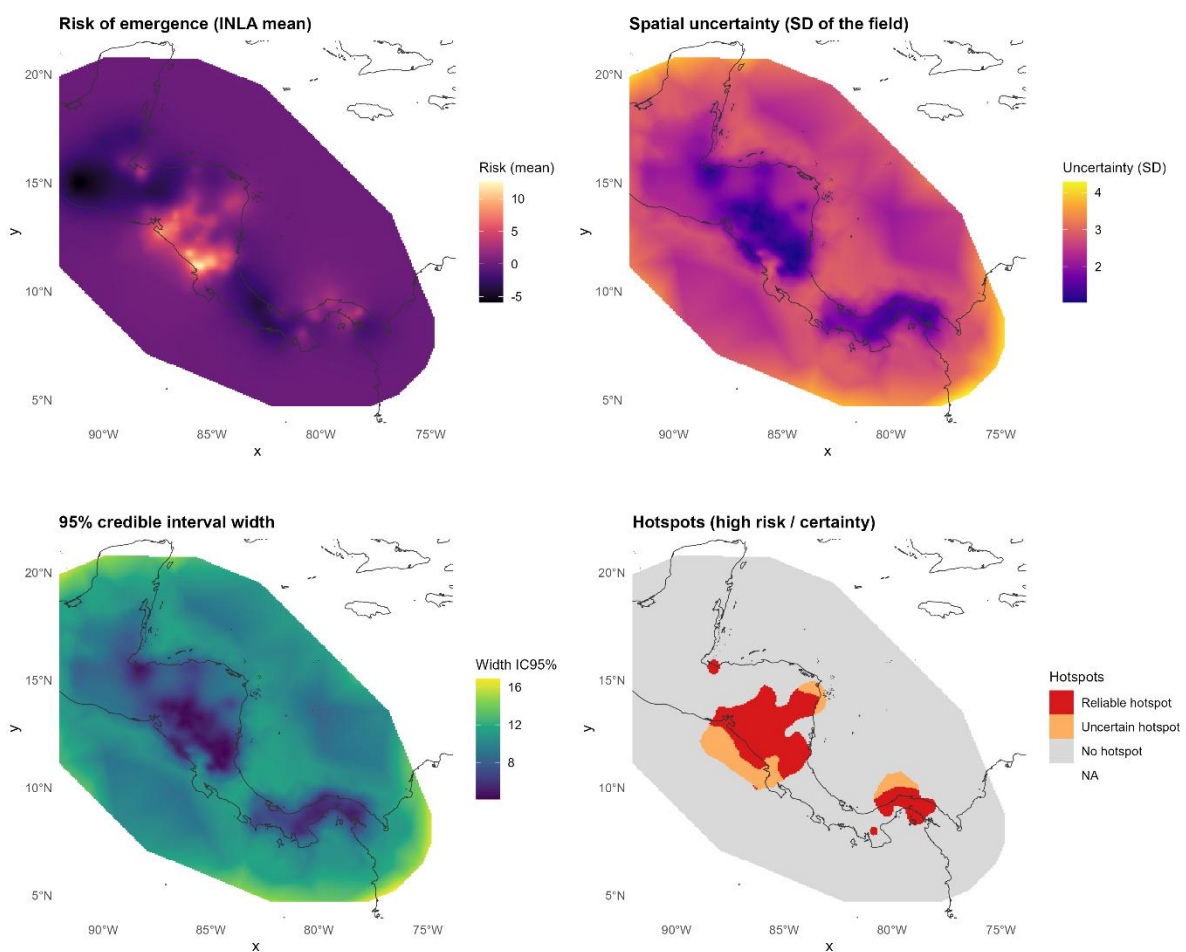
636

637

638

639

640 **Figure 2:** Spatial predictions of *Cochliomyia hominivorax* emergence risk and associated
641 uncertainty. Panels show (top left) the posterior mean of emergence risk estimated using the INLA
642 model, (top right) the spatial uncertainty expressed as the standard deviation of the latent field,
643 (bottom left) the width of the 95% credible interval, and (bottom right) the resulting hotspot
644 classification combining risk and uncertainty, distinguishing reliable hotspots (high risk and low
645 uncertainty), uncertain hotspots (high risk and high uncertainty), and areas with no detected
646 hotspot.

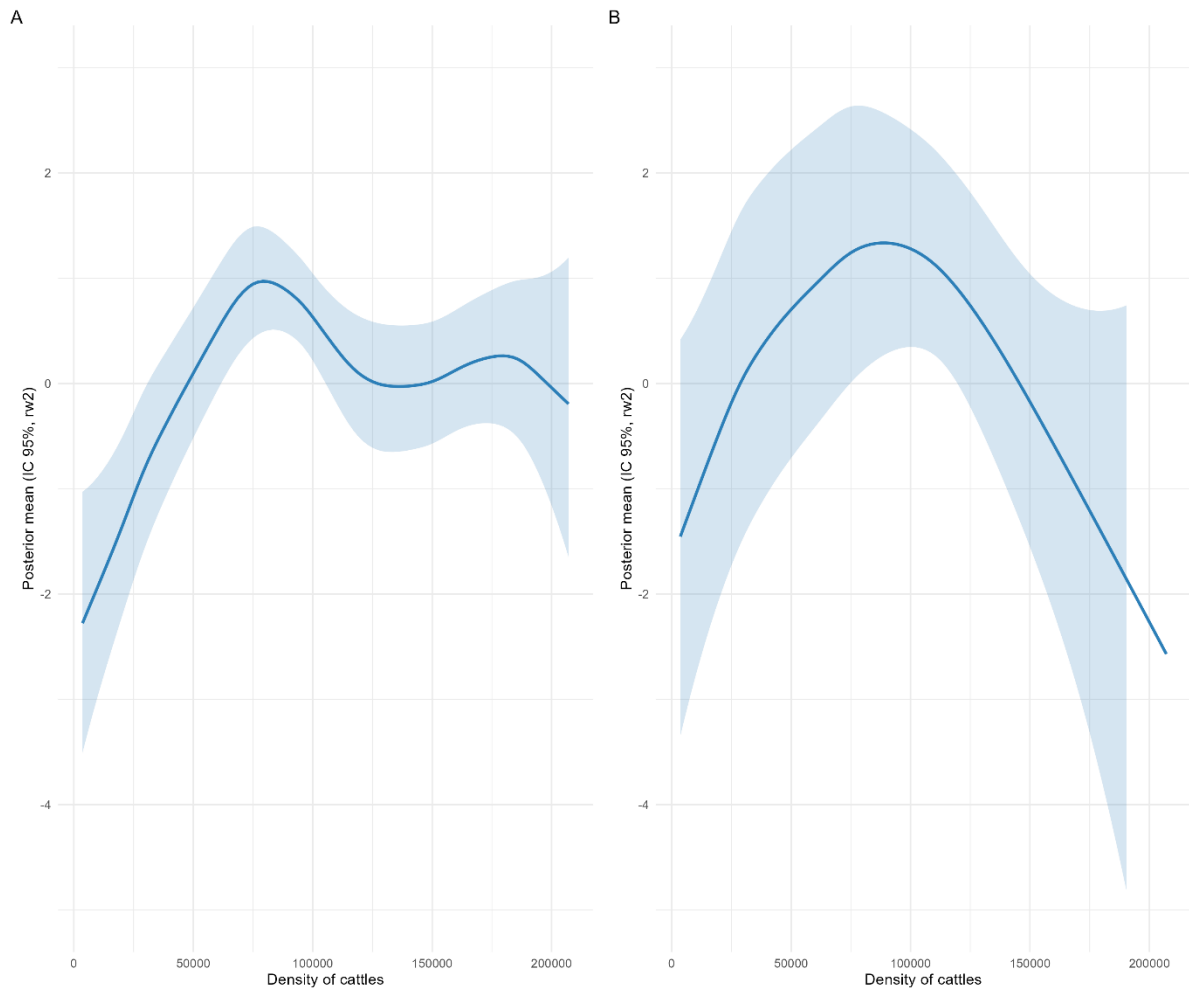


647
648
649
650
651
652
653
654
655

656 **Figure 3:** *Nonlinear effect of cattle density on zoonotic occurrence risk.*

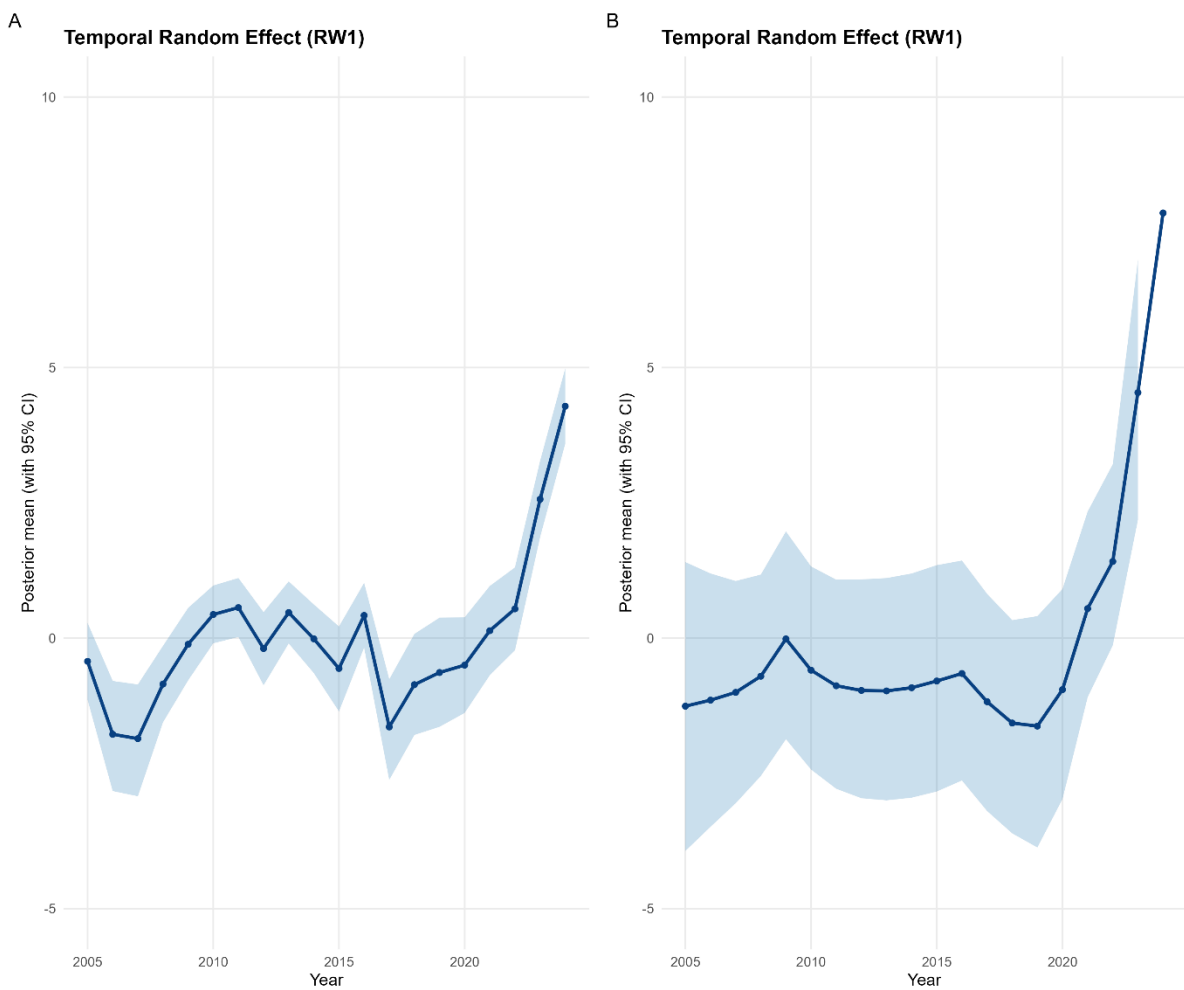
657 (A) Posterior smooth effect of cattle density on the probability of zoonotic diseases (all etiologies
658 combined), estimated using a second-order random walk (RW2) model. (B) Corresponding effect
659 estimated only for *Cochliomyia hominivorax* cases. Solid lines represent the posterior mean and
660 shaded regions show the 95% credible intervals.

661



662
663
664
665
666
667
668
669
670
671
672
673

674 **Figure 4.** Temporal random effects for zoonotic emergence models (RW1). (A) Posterior temporal
675 random effect for the all-zoonoses emergence model, showing moderate inter-annual fluctuations and a
676 gradual long-term increase across the study period, with a sharp rise beginning around 2020. (B)
677 Posterior temporal random effect for the *Cochliomyia hominivorax*-specific model, characterized by
678 near-zero and highly uncertain effects prior to 2018–2020—reflecting the species’ historical
679 near-extinction in Central America—followed by an abrupt and well-supported increase in recent years.
680 Shaded bands represent 95% Bayesian credible intervals (BCIs). Both models were estimated using a
681 first-order random walk (RW1), allowing flexible, data-driven reconstruction of temporal trends.



682

683 **Box 1: From trade-offs to coexistence: A three-dimensional sustainability framework**

684 Reconciling biodiversity conservation with food security and food production is a key sustainability
685 challenge, traditionally framed as a trade-off requiring optimization (Fischer, et al. 2017). Crespin &
686 Simonetti (2021) introduced the concept of *coexistence parameters*, which are the social and ecological
687 factors that can be managed to reduce conflict and shift systems toward states where food security and
688 biodiversity conservation are simultaneously achieved. Such framework conceptualizes the *coexistence*
689 *niche* as an n-dimensional space located at the intersection of food security and biodiversity components
690 (Crespin et Moreira-Arce 2026).

691 However, this two-axis model remains incomplete because it lacks a critical third dimension. related to
692 health. As demonstrated by recent global crises, the drivers of biodiversity loss and food insecurity are
693 inextricably linked to zoonotic risk and public health (Hirst et Halsey 2023). Including zoonotic
694 dynamics within the coexistence model thus highlights a key frontier for sustainability science. This
695 manuscript proposes a theoretical expansion of the *Agroecological Systems Model of Coexistence* by
696 formally integrating a third orthogonal axis-health-aligned with the One Health (OH) paradigm (WHO
697 2022).

698 Adopting the comprehensive OH definition, the new Health axis is deconstructed into three
699 interdependent components that interact with the original two axes: *Human health*, *Animal health*, and
700 *Environmental health*. Human health encompasses physical health (e.g., free from zoonotic diseases)
701 and mental well-being, the latter often derived from "nature's contributions to people" (NCP) (Díaz, et
702 al. 2018). This component interacts directly with food security access (socioeconomic stability) and
703 biodiversity structure (exposure to green spaces). Animal health integrates the physical health and
704 welfare of both domestic and wild animals, recognizing that high stress in animal populations (driven
705 by habitat fragmentation or intensive agriculture) can compromise immunity and increase pathogen
706 shedding (Hayek 2022). Environmental health refers to the integrity of the physical and biological
707 matrix (e.g., soil, water, air) that acts as the foundational "system context" for human and animal health
708 outcomes. For a complete breakdown of the conceptual components, their specific interactions, and
709 potential parameters within the nexus, see Table 1.

710 Identifying the points of intersection between these three axes (see Fig.1) allows us to pinpoint the
711 specific coexistence parameters that simultaneously reduce biodiversity impacts, secure food supplies,
712 and mitigate disease risks. For example, managing connectivity through biological corridors is a key
713 coexistence parameter, it restores environmental health and buffers human health risks by regulating
714 vector populations (Ortiz, et al. 2021) (Prist, et al. 2023), while maintaining crop pollination services
715 (food security). Similarly, diversified agroecological systems act as a coexistence parameter by
716 providing stable food while conserving ecological relations that dilute pathogen prevalence among
717 wildlife reservoirs, thus safeguarding animal health (Crespin et Simonetti 2020).

718 To operationalize this framework, we propose a pragmatic approach grounded in integrated vulnerability
719 mapping. By superimposing data layers for each axis, such as deforestation rates (biodiversity),
720 availability and access indicators (food insecurity) (Sibrian, et al. 2021), and zoonotic risk interfaces
721 (disease burden) (Charles, et al. 2021), we can identify *socio-ecological vulnerability hotspots* where
722 risks converge geographically. This mapping allows us to determine where intervention is most needed
723 to push the local system towards a *basin of coexistence*, a dynamic attractor in phase space where the
724 system remains stable in a state of coexistence despite external shocks (Crespin et Moreira-Arce 2026).
725 By treating human, animal and environmental health as integral components of the coexistence niche,
726 this integration transforms the framework into a comprehensive instrument for regional resilience.

727
728
729

730 **Table 1.** Conceptual axes that interact to create the human-nature coexistence nexus.
 731 Interactions within the nexus can give way to potential coexistence parameters.

Conceptual Axis	Component	Description	Interactions within the Nexus
Biodiversity	1. Compositional	Identity and variety of genes, species, and populations (e.g., pathogen reservoirs, crop varieties).	→ Food Security: Genetic diversity serves as a buffer for crop resilience (Quantity) and dietary diversity (Quality). → Animal Health: Wild populations act as reservoirs; high diversity can dilute pathogen prevalence (dilution effect). → Human Health: Zoonotic spillover risk increases when compositional balance is disrupted (e.g., loss of predators).
	2. Structural	Physical arrangement of habitats (e.g., forest connectivity, patch size, fragmentation).	→ Environmental Health: Intact structures prevent erosion and regulate microclimates. → Human Health: Fragmentation increases "edge effects," heightening human exposure to vectors like ticks/mosquitoes. → Food Security: Landscape structure determines arable land availability and water retention (Quantity).
	3. Functional	Ecological processes (e.g., nutrient cycling, pollination, predation, water filtration).	→ Food Security: Pollination and soil fertility are critical ecosystem services for crop yields (Quantity). → Environmental Health: Water filtration and air purification directly support the "system context" for health. → Animal Health: Predation regulates reservoir populations, preventing disease outbreaks.
Food Security	1. Quantity (Availability)	The supply of food (calories) dependent on production systems and land use.	→ Biodiversity: Expansion of production often degrades Structural biodiversity (deforestation). → Animal Health: Intensification (crowding) increases stress and pathogen transmission in livestock. → Environmental Health: Agrochemical use can degrade soil and water quality.
	2. Quality (Utilization)	Nutritional value, food safety, and diet diversity required for healthy metabolism.	→ Human Health: Adequate nutrition supports immune function (Physical); nutritional deficiencies increase vulnerability to disease. → Biodiversity: Demand for diverse diets encourages the conservation of agrobiodiversity (Compositional) rather than monocultures.
	3. Access & Stability	Physical/economic access to food and the stability of that access over time.	→ Human Health: Poverty and food insecurity drive stress (Mental Health) and reliance on unsafe foods. → Biodiversity: Instability drives coping strategies like bushmeat hunting, impacting wildlife populations (Compositional). → Animal Health: Unregulated trade or hunting compromises wildlife welfare and health.

Health

1. Human Health	Physical: Freedom from disease/injury. Mental: Well-being and resilience.	→ Biodiversity: "Nature's contributions to people" (NCP) support mental well-being (Structural). → Food Security: Healthy populations are economically productive, ensuring stable food access (Access).
2. Animal Health	Physical: Disease status of domestic/wild animals. Welfare: Freedom from distress (Five Freedoms).	→ Biodiversity: Disease outbreaks in wildlife (e.g., chytrid, distemper) can cause extinction events (Compositional). → Food Security: Healthy livestock ensures stable protein supplies; sick animals threaten food safety (Quality).
3. Environmental / Ecosystem Health	Integrity of the physical environment (soil, water, air) that sustains life.	→ Biodiversity: A healthy matrix supports functional ecosystem processes (Functional). → Food Security: Degraded environments (e.g., salinized soil) collapse production systems (Quantity).

732

733

734

735

736 **Box 2. Glossary of concepts for the expanded Coexistence Nexus Framework.** The
 737 following terms are fundamental to the expanded conceptual model presented in Box 1 and
 738 detailed in Table 1.

<i>Term</i>	<i>Definition</i>
Agroecological Systems Model of Coexistence	The original conceptual framework that established the Food-Biodiversity nexus, composed of two multidimensional axes (Food Security and Biodiversity), which this manuscript expands upon (Crespin & Simonetti 2021).
Coexistence Niche	A multi-dimensional subspace where both food production and biodiversity conservation needs are met. It is an n-dimensional space located at the intersection of various components of food security and biodiversity (Crespin & Moreira-Arce 2026).
Coexistence Parameters	Social and ecological factors that can be actively managed to reduce conflict and shift a social-ecological system toward a state where food security and biodiversity are simultaneously achieved (Crespin & Simonetti 2021).
Coexistence Nexus	The expanded conceptual framework resulting from formally integrating the third orthogonal axis of Health (One Health) into the original Food-Biodiversity nexus (Crespin & Moreira-Arce 2026).
One Health (OH)	A comprehensive approach recognizing that the health of humans is inextricably linked to the health of animals and the environment (One Health High-Level Expert Panel et al. 2022).
Human Health	A component of the Health axis encompassing both physical health (e.g., freedom from zoonotic diseases) and mental well-being, the latter often derived from "nature's contributions to people" (NCP) (Díaz et al. 2018).
Animal Health	A component of the Health axis that integrates the physical health and welfare of both domestic and wild animals, including their disease status and freedom from distress and fear (One Health High-Level Expert Panel et al. 2022).
Environmental/Ecosystem Health	A component of the Health axis referring to the integrity of the physical and biological matrix (e.g., clean water, soil stability) that acts as the foundational "system context" for all other health outcomes (One Health High-Level Expert Panel et al. 2022).
Socio-ecological vulnerability hotspots	Specific geographic locations identified by integrated vulnerability mapping where critical risks from biodiversity erosion, food insecurity, and disease burden converge, requiring targeted intervention.
Basin of Coexistence	Not a physical place, but a dynamic attractor in phase space where a social-ecological system remains stable in a desired state of coexistence despite external shocks or perturbations (Crespin & Moreira-Arce 2026).

739
 740
 741
 742
 743
 744
 745